Korean J. Chem. Eng., 35(8), 1710-1715 (2018)
DOI: 10.1007/s11814-018-0072-2

pISSN: 0256-1115
eISSN: 1975-7220

Solid-liquid phase equilibria, excess molar volume, and molar refraction deviation for the mixtures of ethanoic acid with propanoic, butanoic, and pentanoic acid

Kyeong-Ho Lee, Ji-Eun Gu, Ha-Young Oh, and So-Jin Park†

Department of Chemical Engineering and Applied Chemistry, College of Engineering,
Chungnam National University, Daejeon 34134, Korea
(*Received 27 February 2018 • accepted 30 April 2018*)

Abstract−The paper reports the solid-liquid phase equilibria (SLE), excess molar volume (V^E), and molar refraction deviation (ΔR) for binary systems of ethanoic acid with the C_3 to C_5 carboxylic acids, propanoic, butanoic, and pentanoic acid, which are the main constituents of bio-butanol fermentation broth. The SLE was determined via a synthetic method using a custom-built glass tube at atmospheric pressure, whereas the thermodynamic mixture properties, V^E and ΔR were obtained from directly measured density and refractive index using a precision densitometer and refractometer, respectively. All of the SLE that were determined for binary mixtures of ethanoic acid+C_3-C_5 carboxylic acids showed a single eutectic point and regressed well with the NRTL activity model within 0.6 K of RMSD. The V^E values for the same binaries were positive for the entire composition ranges of all the systems, whereas the ΔR values were negative for all the systems. The V^E and ΔR were well regressed by polynomial equations, namely Redlich-Kister within 0.006 $cm^3 \cdot mol^{-1}$ of the standard deviation for V^E and 0.02 $cm^3 \cdot mol^{-1}$ for ΔR.

Keywords: SLE, V^E, ΔR, Carboxylic Acid, Bio-butanol

INTRODUCTION

Even though bioethanol and biodiesel were considered as transportation fuels for early heat engines of vehicles, they were largely forgotten once fossil fuels were introduced as cheap, reliable and convenient transportation fuels. However, biofuels have been regaining their popularity owing to the need for renewable resources and the high cost of petroleum feedstock together with a growing concern about global warming and the need for energy independence [1]. In fact, these preferences are not surprising because fossil fuels are essentially biofuels formed because of the subterraneous decomposition of plants. Many countries around the world are using biofuels, mainly bioethanol and biodiesel. A relatively new biofuel with four carbon atoms, bio-butanol, has shown promise because of its advantages compared to bioethanol: a favorable higher energy density (29.2×10^6 $kJ \cdot m^{-3}$), compatibility with gasoline, lower corrosiveness, and less emissivity of the hydrocarbon carbon monoxide and NO_x, etc. [2].

Commercial problems associated with the bio-butanol fermentation process are mainly the high feedstock cost, very low butanol yield caused by severe product inhibition during bioprocessing and increased separation cost, etc. [3]. Many attempts to enhance the fermentation yields by modification of the microorganism and the use of alternative more affordable forms of renewable biomass, such as agricultural waste and wood chips [4], have been reported, even though it should be a long-term project. The other topic is the development of economical separation technology for the fermentation product. Extensive reviews of technologies for the separation process of conventional ABE (acetone-butanol-ethanol) fermentation products have been conducted. Among them, a process consisting of liquid extraction, membrane pervaporation, adsorption, gas stripping, vacuum distillation, and membrane extraction was largely considered. In industry, equilibrium-staged separation technologies are still popular, and it can therefore be concluded that solvent extraction, adsorption, and membrane pervaporation, are the most efficient processes from an energy perspective [5]. However, the related process design data were still not optimal, even though they are indispensable for developing such an equilibrium-staged separation process.

We studied in this work the related phase equilibrium and thermodynamic properties for the development of the separation process. Extensive phase equilibrium data for acetone, butanol, and ethanol, the main fermentation products of the ABE process, are available [6-12]. However, there is still a lack of data, in particular, some of the side products such as C_2-C_4 carboxylic acids and some of the alcohols that complicate the separation process. The usual ABE fermentation process first produces butanoic, propanoic, and ethanoic acids by *C. acetobutylicum*. Therefore, we studied systematically the related phase equilibrium and mixture property data for the systems containing C_2-C_4 carboxylic acid and those of the C_5 acid and other byproduct components.

More specifically, we determined the solid-liquid phase equilibria (SLE) data for binary systems, ethanoic acid with propanoic, butanoic, and pentanoic acid, respectively. These data are important mainly for crystallization process design, the solvent selection of reaction mixtures, and safety assessment. In addition, the excess molar volume and molar refraction deviation for the same binary mixtures at 298.15 K were determined from measured thermody-

†To whom correspondence should be addressed.
E-mail: sjpark@cnu.ac.kr

Table 1. Gas-chromatographic analysis and properties of the chemicals

Substance	Purity (wt%)	M.W. (g/mol)	Melting point (K)		ρ/g cm^{-3} at 298.15 K[a]		n_D at 298.15 K[b]	
			Exp.	Ref.	Exp.	Ref.	Exp.	Ref.
Ethanoic acid	>99.9	60.05	289.31	289.84[c]	1.04774	1.04395[e]	1.3729	1.36969[e]
Propanoic acid	>99.9	74.08	252.34	252.3[d]	0.98945	0.98833[e]	1.3846	1.38484[e]
Butanoic acid	>99.9	88.11	268.01	267.9[d]	0.95349	0.95317[e]	1.3967	1.39599[e]
Pentanoic acid	>99.9	102.13	240.69	238.7[d]	0.93549	0.93485[f]	1.4065	1.40641[f]

[a]Standard uncertainties u(ρ)=5×10^{-5} g·cm^3, u(T)=0.01 K
[b]Standard uncertainties u(n_D)=2×10^{-4}, u(T)=0.05 K
[c]Ref. [9]. [d]Ref. [10]. [e]Ref. [11]. [f]Ref. [12]

namic mixture densities (ρ) and refractive indices (n_D). The SLE data were then regressed with two common activity coefficient models: NRTL [13] and UNIQUAC [14], whereas the excess molar volume and molar refraction deviation were regressed with the Redlich-Kister model [15].

EXPERIMENT

1. Materials

The substances used in our experiments were ethanoic acid (Samchun Pure Chemical Co., Korea). Propanoic (K and P are a capital) acid (Sigma-Aldrich, USA), butanoic acid (Junsei Chemical Co., Japan), and pentanoic acid (Alfa Aesar, USA). The mass fraction of each substance was more than 0.999 by gas chromatographic analysis. All the used chemicals were dried with 3 Å pellet type molecular sieves. The water content of the chemicals was analyzed less than 5×10^{-5} g·g^{-1} by Metrohm 684 KF-Coulometer. The determined density and refractive index of used substances are provided in Table 1 along with the literature reported values [11,12].

2. Experimental Apparatus and Procedure

SLE determination involved using a cryostat and custom-built triple-glass jacketed still, in which the melting or freezing process of a solid sample can be visually observed. The outermost exterior glass column of the glass jacket was maintained under vacuum to prevent moisture from freezing on the surface. The cooling/heating media were circulated through the center jacket of the glass still. The innermost equilibrium cell was not only heated or cooled but also insulated from the environment via the circulated cooling/heating media. The equilibrium cell was purged with nitrogen gas for dehumidification [16,17]. The equilibrium point between the solid and liquid for the given composition was visually checked when the last crystal of the sample mixture disappeared. The SLE temperature was determined with a precision temperature measuring system (ASL F250, UK). The standard uncertainty due to the repeatability of the SLE temperature determination was estimated to be less than ±0.05 K. The mole fraction of each of the binary samples was calculated gravimetrically using a microbalance (A&D, Japan). The standard uncertainty due to the repeatability of the determined mole fraction was estimated to be less than ±2×10^{-4}.

The ρ of the pure and mixture components under atmospheric pressure was determined directly using a oscillating U-tube densimeter (Anton Paar model DMA 5000) and V^E was calculated from the measured ρ. The U-tube densimeter was calibrated using standard bi-distilled water and dried air before every measurement. According to the manufacturer's specification, the accuracy of measured density is better than 5×10^{-6} g cm^{-3} in the ranges of 0 and 3 g cm^{-3} and the temperature is ±0.01 K. The samples were prepared gravimetrically in a stoppered glass vials using a microbalance. The high-boiling-point component was first added to the vial to minimize evaporation losses. The estimated systematic uncertainty in the mass and density measurements was less than 2×10^{-4} in the mole fraction and 5×10^{-5} g cm^{-3} for the density, respectively.

The refractive index (n_D) was determined with a digital precision refractometer (KEM, model RA-520N, Kyoto, Japan). The stated accuracy by manufacturer is to be ±5×10^{-5} and ±1×10^{-4} in the refractive indices of 1.32-1.40 and 1.40-1.58, respectively. The temperature accuracy is ±5×10^{-2} K. The systematic uncertainty in the n_D determination was estimated to be less than 2×10^{-4}. The values of ΔR were obtained from the measured n_D data. The reproducibility of the measurement was checked with bi-distilled water. The detailed experimental procedure of ρ and n_D has been described elsewhere [18,19].

RESULTS AND DISCUSSION

The simplified SLE equation without considering of solid-solid phase transition is as follows: [20]

$$x_i = \frac{1}{\gamma_i}\left[\exp\left\{\frac{\Delta H^{fus}(T_{mi})}{R}\left(\frac{1}{T_{mi}}-\frac{1}{T}\right)\right\}\right] \quad (1)$$

where x_i, γ_i is the liquid phase mole fraction and the activity coefficient of component i, respectively. T_{mi} is the absolute melting temperature and $\Delta H^{fus}(T_{mi})$ is the molar enthalpy of fusion at the temperature of T_{mi}. R is the universal gas constant. The experimentally measured SLE data for the binary systems consisting of ethanoic acid with propanoic, butanoic, and pentanoic acid are presented in Table 2 and illustrated in Figs. 1 to 3, respectively. As shown, all the determined systems in this work show a single eutectic point. The experimental SLE data were optimized with a common activity coefficient model: NRTL and UNIQUAC model equation. The solid lines represent the recalculated data from the optimized model parameters. The NRTL model gives slightly better optimization results than the UNIQUAC model for all the determined systems.

Table 2. The experimental SLE data for the ethanoic acid+propanoic, butanoic and pentanoic acid systems

Systems	x_1	T/K	x_1	T/K
{Ethanoic acid (1) +propanoic acid (2)}	0.0000	252.34	0.4000	241.84
	0.0500	248.87	0.5000	251.45
	0.1001	246.83	0.6000	260.85
	0.2002	241.82	0.7000	268.82
	0.2801	238.36	0.8001	276.47
	0.2999	236.85	0.8987	283.05
	0.3199	236.04	0.9500	286.21
	0.3447	235.88	1.0000	289.31
	0.3634	238.15	-	-
{Ethanoic acid (1) +butanoic acid (2)}	0.0000	268.01	0.4401	250.02
	0.0499	265.40	0.5002	254.86
	0.1002	262.95	0.5999	262.65
	0.2004	257.79	0.7012	269.95
	0.3001	252.65	0.7990	276.47
	0.3705	248.18	0.9019	282.96
	0.3899	246.85	0.9500	285.89
	0.4050	245.65	1.0000	289.31
	0.4101	246.53	-	-
{Ethanoic acid (1) +pentanoic acid (2)}	0.0000	240.69	0.3999	246.53
	0.0505	239.54	0.5000	254.35
	0.1000	237.73	0.6000	261.92
	0.1557	236.22	0.7008	270.28
	0.2006	234.34	0.8000	277.36
	0.2199	233.95	0.9001	283.12
	0.2400	234.79	0.9500	286.10
	0.2701	237.27	1.0000	289.31
	0.3016	239.94	-	-

Standard uncertainties u(x)=0.0002, u(T)=0.05 K

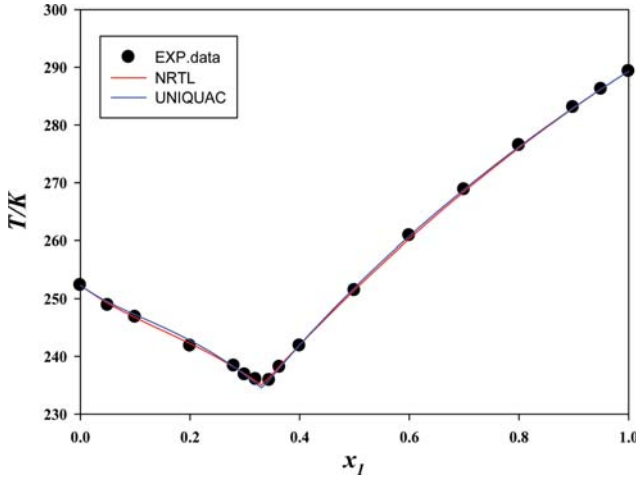

Fig. 1. The experimental SLE diagram for the system {ethanoic acid (1)+propanoic acid (2)} (●).

The optimized NRTL, UNIQUAC model parameters and the root-mean-square deviation (RMSD) from Eq. (2) are listed in Table 3. The RMSD was less than 0.6 K for all of determined systems.

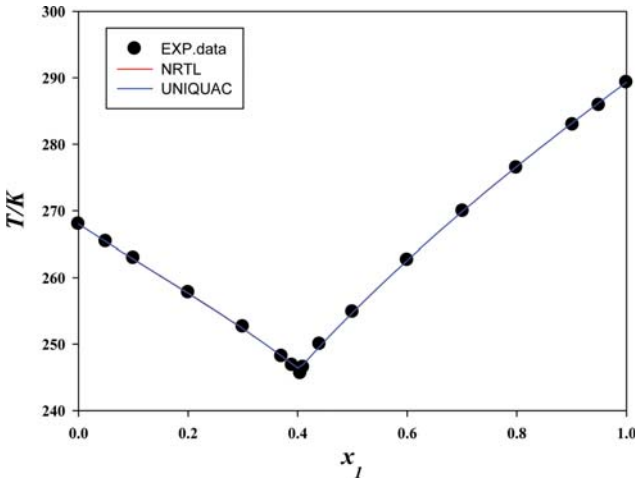

Fig. 2. The experimental SLE diagram for the system {ethanoic acid (1)+butanoic acid (2)} (●).

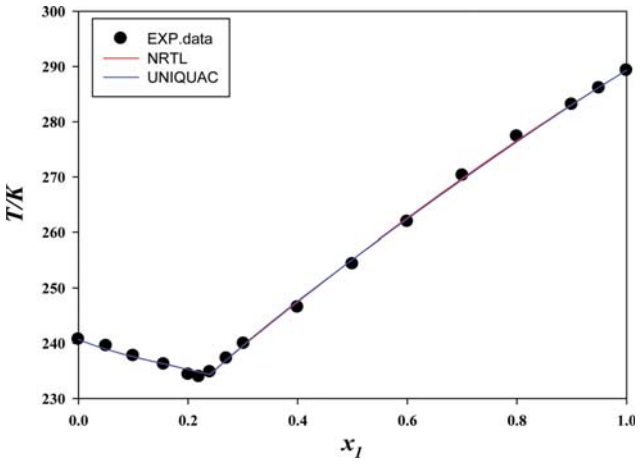

Fig. 3. The experimental SLE diagram for the system {ethanoic acid (1)+pentanoic acid (2)} (●).

$$\mathrm{RMSD}=\left[\frac{\Sigma_i\Sigma_\alpha\Sigma_k(x_{ik}^{\alpha(exp)}-x_{ik}^{\alpha(cal)})}{6N}\right]^{1/2} \quad (2)$$

The exact eutectic points were estimated with the NRTL equation, and on the basis of the NRTL parameters, they are x_1=0.3305/T=234.94 K, x_1=0.4026/T=246.26 K and x_1=0.2400/T=234.33 K for the binary systems of ethanoic acid with propanoic acid, butanoic acid, and pentanoic acid, respectively. The standard uncertainty due to repeatability of the SLE temperature determination was estimated to be less than ±0.05 K.

The determined V^E and ΔR for the same binary mixtures are listed in Table 4 with the measured ρ and n_D for pure component and mixtures at 298.15 K.

$$V^E/\mathrm{cm}^3\cdot\mathrm{mol}^{-1}=\frac{\Sigma_i x_i M_i}{\rho_m}-\Sigma_i\left[\frac{x_i M_i}{\rho_i}\right] \quad (3)$$

where ρ_i, ρ_m and M_i are the densities of the pure and mixture components, and the molar mass, respectively. The experimental V^E

Table 3. The adjustable model parameters and the RMSD for each binary system

Models	Systems	A_{ij}/cal·mol^{-1}	A_{ji}/cal·mol^{-1}	α	RMSD
NRTL	{Ethanoic acid (1)+propanoic acid (2)}	−1504.92	2550.79	0.10	0.27
	{Ethanoic acid (1)+butanoic acid (2)}	−292.433	576.268	0.34	0.28
	{Ethanoic acid (1)+pentanoic acid (2)}	−448.973	1203.37	0.29	0.59
UNIQUAC	{Ethanoic acid (1)+propanoic acid (2)}	−399.095	896.458	-	0.40
	{Ethanoic acid (1)+butanoic acid (2)}	−253.267	452.951	-	0.28
	{Ethanoic acid (1)+pentanoic acid (2)}	−340.810	827.698	-	0.62

Table 4. The experimental densities, excess molar volumes, refractive indices, and molar refraction deviation for the carboxylic acid systems at 298.15 K

x_1	ρ/g cm^{-3}	V^E/cm^3 mol^{-1}	n_D	ΔR/cm^3 mol^{-1}
Ethanoic acid (1)+propanoic acid (2)				
0.0738	0.99262	0.0133	1.3839	−0.0886
0.0996	0.99372	0.0207	1.3836	−0.1178
0.1994	0.99816	0.0443	1.3823	−0.2282
0.2997	1.00289	0.0656	1.3809	−0.3103
0.4101	1.00847	0.0823	1.3794	−0.3685
0.5002	1.01339	0.0877	1.3783	−0.3863
0.6003	1.01927	0.0853	1.3768	−0.3817
0.7002	1.02561	0.0743	1.3754	−0.3410
0.8002	1.03249	0.0535	1.3741	−0.2589
0.8991	1.03975	0.0311	1.3724	−0.1541
0.9505	1.04375	0.0152	1.3718	−0.0711
Ethanoic acid (1)+butanoic acid (2)				
0.0505	0.95608	0.0401	1.3958	−0.1320
0.1003	0.95877	0.0755	1.3948	−0.3388
0.1996	0.96450	0.1429	1.3928	−0.7039
0.3006	0.97103	0.1938	1.3907	−0.9960
0.4006	0.97822	0.2316	1.3885	−1.2086
0.5030	0.98655	0.2491	1.3861	−1.3275
0.6052	0.99593	0.2494	1.3836	−1.3297
0.7001	1.00588	0.2264	1.3813	−1.2138
0.7998	1.01779	0.1802	1.3786	−0.9517
0.9001	1.03156	0.1108	1.3757	−0.5176
0.9499	1.03928	0.0607	1.3744	−0.2237
Ethanoic acid (1)+pentanoic acid (2)				
0.0486	0.93789	0.0610	1.4057	−0.3784
0.0999	0.94061	0.1171	1.4044	−0.7888
0.1998	0.94638	0.2215	1.4018	−1.4939
0.3000	0.95306	0.2993	1.3987	−2.1039
0.3997	0.96078	0.3482	1.3962	−2.5198
0.5000	0.96973	0.3775	1.3932	−2.7780
0.6075	0.98107	0.3755	1.3892	−2.8581
0.7001	0.99245	0.3557	1.3865	−2.6334
0.8002	1.00727	0.2883	1.3815	−2.1817
0.9002	1.02524	0.1784	1.3769	−1.3094
0.9502	1.03613	0.0825	1.3746	−0.6958

Standard uncertainties u(x)=0.0002, u(ρ)=5×10^{-5} g·cm^3, u(n_D)=2×10^{-4}

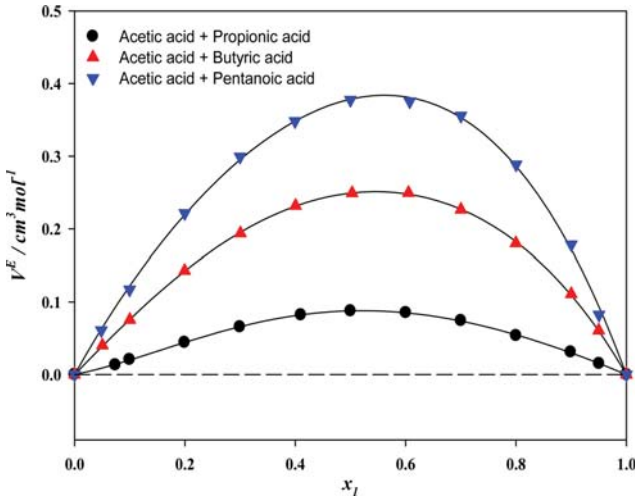

Fig. 4. V^E (cm^3·mol^{-1}) for the binary systems at 298.15 K; ●, {ethanoic acid (1)+propanoic acid (2)}; ▲, {ethanoic acid (1)+butanoic acid (2)}; ▼, {ethanoic acid (1)+pentanoic acid (2)}; solid curves were calculated data from the Redlich-Kister parameters.

values show positive deviation from ideality as illustrated in Fig. 4. Actually, the smaller carboxylic acids (carbon number of 1-5) are polar and participate in hydrogen bonding, since they are both hydrogen bond acceptors and donors at the same time. However, their mixtures show a positive deviation of V^E values, possibly caused by the relatively low dielectric constant of these carboxylic acids. The dielectric constants of the small carboxylic acids are relatively low: ethanoic acid, 6.20; propanoic acid, 3.10; butanoic acid, 2.80; pentanoic acid, 2.60. These low dielectric constants suggest that the influence of the non-polar alkyl group dominates the influence of the carboxyl group in carboxylic acid. Therefore, the positive deviation increased by increasing the carbon atom number of the second component of carboxylic acid. Furthermore, the ΔR of all the systems was negative, and the negativity increases as the difference in molecular weight in the binary mixtures increases as shown in Fig. 5. Namely, the negativity of deviation increases in the order of ethanoic acid+propanoic<ethanoic acid+butanoic acid< ethanoic acid+pentanoic acid.

The values of ΔR were obtained from Eq. (4) using R_m, R_i, and ϕ_i [21]:

$$\Delta R/cm^3 \cdot mol^{-1} = R_m - \Sigma_i \phi_i R_i \quad (4)$$

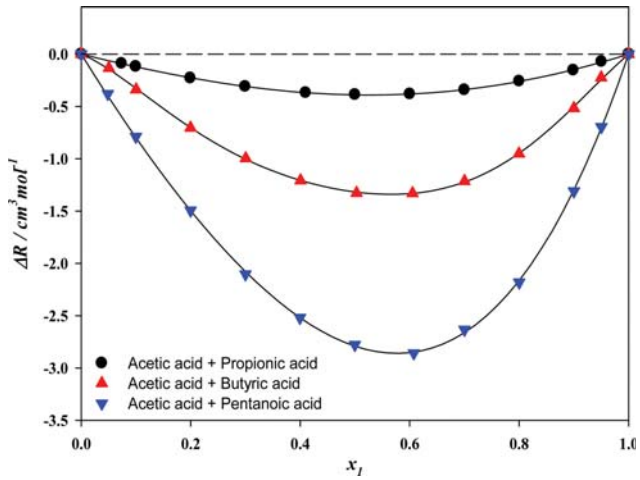

Fig. 5. ΔR ($cm^3 \cdot mol^{-1}$) for the binary systems at 298.15 K; ●, {ethanoic acid (1)+propanoic acid (2)}; ▲, {ethanoic acid (1)+butanoic acid (2)}; ▼, {ethanoic acid (1)+pentanoic acid (2)}; solid curves were calculated data from the Redlich-Kister parameters.

$$R_m = \left[\frac{n_D^2 - 1}{n_D^2 + 1}\right]\left[\frac{\Sigma_i x_i M_i}{\rho_m}\right] \quad (5)$$

$$R_i = \left[\frac{n_{D,i}^2 - 1}{n_{D,i}^2 + 1}\right]\left[\frac{M_i}{\rho_i}\right] \quad (6)$$

$$\phi_i = \frac{x_i V_i}{\Sigma_j x_j V_j} \quad (7)$$

where R_m and R_i are the molar refractivity of the mixture components and pure component i, respectively. ϕ_i is the volume fraction of the pure component i in the mixture. n_D, $n_{D,i}$ are the refractive index for the mixture and the pure component i, respectively. V_i is the molar volume of the pure component i.

The determined V^E and ΔR values were regressed with the following Redlich-Kister equation.

$$V^E, \Delta R = x_1 x_2 \Sigma_{i=1}^{n} A_i (x_1 - x_2)^{i-1} \quad (8)$$

where x, A_i, and n is the mole fraction, fitted Redlich-Kister parameter, and the number of fitted parameters, respectively.

The Akaike Information Criteria (AIC) [22], Eq. (9) was used to optimize the number of Redlich-Kister parameters

$$AIC = nD \ln SSR + 2nP \quad (9)$$

where nD, SSR, and nP means the number of data points, the sum of squares of the residuals and the number of parameters, respectively. For convenient application, we only considered at most seven Redlich-Kister parameters for AIC evaluation.

The fitted parameters and their corresponding standard deviations, σ_{st}, are tabularized in Table 5. The σ_{st} is defined as:

$$\sigma_{st} = \sqrt{\frac{\Sigma_i^n (E_i^{calc} - E_i^{exp})^2}{(N - n)}} \quad (10)$$

where E_i^{cal} is the recalculated values with fitted parameters and E_i^{exp} is experimental values of component i. N and n are the experimental data points and the number of Redlich-Kister model parameters, respectively.

The mean deviations of the V^E values were 0.0008, 0.0015, and 0.0056 $cm^3 \cdot mol^{-1}$ for the {ethanoic acid+propanoic acid}, {ethanoic acid+butanoic acid} and {ethanoic acid+pentanoic acid} mixtures, respectively. On the other hand, ΔR is 0.0037, 0.0144, and 0.0191 $cm^3 \cdot mol^{-1}$ for the {ethanoic acid+propanoic acid}, {ethanoic acid+butanoic acid} and {ethanoic acid+pentanoic acid} mixtures, respectively.

CONCLUSIONS

The SLE determined for the mixtures {ethanoic acid+C_3-C_5 monocarboxylic acid} exhibit a single eutectic point. The eutectic points estimated by the NRTL activity coefficient model are x_1=0 0.3305/T=234.94 K, x_1=0.4026/T=246.26 K and x_1=0.2400/T=234.33 K for the systems ethanoic acid+propanoic acid, ethanoic acid+butanoic acid, and ethanoic acid+pentanoic acid, respectively. They regressed well with the NRTL model within 0.6 K of RMSD. The densities, refractive indices, and excess and deviation properties of the C_2-C_5 monocarboxylic acid mixtures were determined at 298.15 K. The values of V^E were positive for the entire composition ranges of all the determined carboxylic acid mixture systems, whereas the values of ΔR were entirely negative for the same systems. The positivity of the V^E values increased in a regular way as the carbon number in the monocarboxylic acids increased. Similarly, the negativity of ΔR also increased as the carbon number in the constituent carboxylic acid increased. These results could be explained with aspect of the intermolecular interaction and molecular size and structure. The low dielectric constant of the C_2-C_5 monocarboxylic acid caused the V^E values to be positive, i.e., the non-polarity of the alkyl group dominates the low polarity of the carboxyl group in carboxylic acid. Moreover, apart from the interaction among constituent molecules, the difference in molecular

Table 5. Adjustable parameters of Redlich-Kister (A_i) and standard deviations of V^E and ΔR at 298.15 K

	Systems	A_1	A_2	A_3	A_4	A_5	σ_{st}/cm^3 mol^{-1}
V^E	Ethanoic acid (1)+propanoic acid (2)	0.3512	0.0388	−0.1151	0.0460	-	0.0008
	Ethanoic acid (1)+butanoic acid (2)	0.9963	0.1761	0.0511	0.0885	-	0.0015
	Ethanoic acid (1)+pentanoic acid (2)	1.5140	0.3475	0.1883	-	-	0.0056
ΔR	Ethanoic acid (1)+propanoic acid (2)	−1.5585	−0.1828	0.1027	-	-	0.0037
	Ethanoic acid (1)+butanoic acid (2)	−5.2685	−1.3384	−0.6380	0.1894	2.6231	0.0144
	Ethanoic acid (1)+pentanoic acid (2)	−11.1654	−3.4743	−0.7620	-	-	0.0191

size and structure also results in negative ΔR values. The Redlich-Kister model regressed very well the experimental data within standard deviation of 0.006 $cm^3 \cdot mol^{-1}$ for V^E and 0.02 $cm^3 \cdot mol^{-1}$ for ΔR, respectively.

ACKNOWLEDGEMENTS

This work was granted financial support from the research fund of Chungnam National University.

REFERENCES

1. P. H. Pfromm, V. Amanor-Boadu, R. Nelson, P. Vadlani and R. Madl, *Biomass Bioenergy*, **34**, 515 (2010).
2. C. Hergueta, M. Bogarra, A. Tsolakis, K. Essa and J. M. Herreros, *Fuel*, **208**, 662 (2017).
3. Y. S. Jang, A. Malaviya, C. H. Cho, J. M. Lee and S. Y. Lee, *Bioresour. Technol.*, **123**, 653 (2012).
4. K. Karimi, M. Tabatabaei, I. S. Horvath and R. Kumar, *Biofuel Res. J.*, **301** (2015).
5. S. Xie, C. Yi and X. Qiu, *J. Chem. Eng. Data*, **58**, 3297 (2013).
6. D. Rabari and T. Banerjee, *Fluid Phase Equilib.*, **355**, 26 (2013).
7. S. Zheng, H. Cheng, L. Chen and Z. Qi, *J. Chem. Thermodynam.*, **93**, 127 (2016).
8. G. H. Lee and S. J. Park, *Fluid Phase Equilib.*, **436**, 47 (2017).
9. I. Malijevska, *Fluid Phase Equilib.*, **211**, 257 (2003).
10. M. Tadie, I. Bahadur, P. Reddy, P. T. Ngema, P. Naidoo, N. Deenadayalu and D. Ramjugernath, *J. Chem. Thermodynam.*, **57**, 485 (2013).
11. K. Granados, J. Gracia-Fadrique, A. Amigo and R. Bravo, *J. Chem. Eng. Data*, **51**, 1356 (2006).
12. I. Bahadur, S. Singh, N. Deenadayalu, P. Naidoo and D. Ramjugernath, *Thermochi. Acta*, **590**, 151 (2014).
13. H. Renon and J. M. Prausnitz, *AIChE J.*, **14**, 135 (1968).
14. D. Abrams and J. M. Prausnitz, *AIChE J.*, **21**, 116 (1975).
15. O. Redlich and A. T. Kister, *Ind. Eng. Chem.*, **40**, 345 (1948).
16. S. H. Shin, I. H. Jeong, Y. S. Jeong and S. J. Park, *Fluid Phase Equilib.*, **376**, 105 (2014).
17. S. H. You, I. H. Jeong, I. C. Hwang and S. J. Park, *Fluid Phase Equilib.*, **383**, 21 (2014).
18. S. J. Park, R. H. Kwon and Y. Y. Choi, *Fluid Phase Equilib.*, **361**, 130 (2014).
19. I. Y. Jeong, R. H. Kwon, S. J. Park and Y. Y. Choi, *J. Chem. Eng. Data*, **59**, 289 (2014).
20. A. Jakob, R. Joh, C. Rose and J. Gmehling, *Fluid Phase Equilib.*, **113**, 117 (1995).
21. T. M. Aminabhavi and B. Gopalakrishna, *J. Chem. Eng. Data*, **40**, 856 (1995).
22. H. Akaike, *IEEE Trans. Automat. Contr.*, **AC-19**, 716 (1974).